RSC Advances

ROYAL SOCIETY OF CHEMISTRY

www.rsc.org/advances

We have studied the soybean seed ferritin stabilized rutin nanodispersions with improved water-solubility, thermal stability, and UV radiation stability.

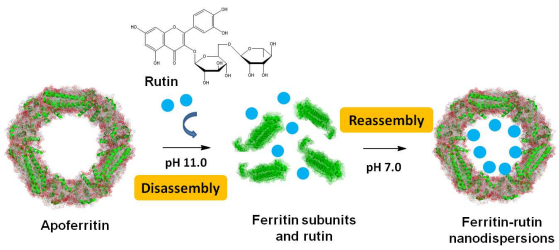

Synthesis of Homogeneous Protein-Stabilized Rutin Nanodispersions by Reversible Assembly of Soybean (*Glycine max*) Seed Ferritin

Rui Yang[a], *Zhongkai Zhou*[a,*], *Guoyu Sun*[a], *Yunjing Gao*[a], *Jingjing Xu*[a], *Padraig Strappe*[b,c], *Chris Blanchard*[b,c], *Yao Cheng*[a], *Xiaodong Ding*[a]

[a] *Key Laboratory of Food Nutrition and Safety, Ministry of Education, Tianjin University of Science and Technology, Tianjin 300457, China.*

[b] *School of Biomedical Sciences, Charles Sturt University, WaggaWagga, NSW 2678, Australia*

[c] *ARC Functional Grains Centre, Charles Sturt University, Wagga Wagga. NSW 2678, Australia*

*Corresponding authors

Prof. Zhongkai Zhou (PhD)

School of Food Engineering and Biotechnology,

Tianjin University of Science and Technology, Tianjin, 300457, China.

Phone +862260601408

Fax +862260601371

E-mail: zkzhou@tust.edu.cn

Abstract

Rutin is a common dietary flavonoid with important pharmacological activities. However, its application in the food industry is limited mainly because of its poor water-solubility. The nano-scale ferritin cage provides an ideal space for subtle encapsulation of hydrophobic rutin molecules. This study describes the preparation of novel homogeneous soybean seed ferritin stabilized rutin nanodispersions (FRNs) by a unique reversible dissociation and reassembly of the apoferritin. The characteristics including the water-solubility, morphology, leakage kinetics, and stability of the FRNs were investigated. Results indicated that the rutin molecules could be successfully encapsulated within the protein cages with a rutin/protein molar ratio of 30.1 to 1, and the encapsulation and loading efficiency were 25.1% (w/w) and 3.29% (w/w), respectively. *In vitro* experiments of rutin release demonstrated that the entrapment of rutin was effective, with more than 75% (w/w) still encapsulated in the ferritin cage after storage for 15 days. Furthermore, the thermal and UV radiation stability of ferritin trapped rutin was greatly improved due to the encapsulation as compared to free rutin. Additionally, the antioxidant activity of FRNs was partly retained as compared to free rutin molecules. This study provides a novel strategy for the design and fabrication of nanocarriers providing water-insoluble molecules with protection and stabilization.

Key words: Rutin, Ferritin, Solubility, Stability, Nanodispersion

Introduction

The natural rutin molecule (3',4',5,7-tetrahydroxyflavone-3-rutinoside, also known as quercetin-3-O-rutinoside) (Fig. 1A), is a common dietary flavonoid known as vitamin P that is widely consumed through plant-derived beverages and foods and is also prevalent in traditional and folk medicines.[1,2] It has been reported that rutin possesses significant anti-inflammatory, antibacterial, antitumor, anti-ageing, and antioxidant activities which make it a popular ingredient of herbal remedies.[3,4] Rutin contains a natural yellow pigment, and has also been extensively used as a coloring, antioxidant, and flavoring additive in the food industry. However, applications in the food and pharmaceutical industries are limited mainly because of its poor water solubility, which is often associated with low and variable bioavailability and short biological half-life.[5] Novel improvements to enhance the water solubility and stability of rutin would be beneficial.

Recently, micro/nanoencapsulation of poorly water soluble bioactive compounds has attracted attention in the food and pharmaceutical industry in various applications such as protection of bioactivity and controlled release for improving bioavailability.[6,7] Several strategies, such as supramolecular inclusion by cyclodextrins,[8,9] ionotropic gelation,[10] self-emulsifying systems,[11] and lipid-based onion-type multilamellar vesicle entrapment (MLVs)[12] have been successfully used for encapsulating rutin to improve its solubility and stability. However, the encapsulated rutin particles have been reported to be of non-uniform size, which may affect their sensory properties, storage, and bioavailability. In addition, such methods usually require the addition of considerable amounts of surfactants or organic solvents, which may result in sample contamination and environmental pollution.

The soybean seed ferritin (SSF) is a cage like protein, which provides a natural vehicle for encapsulation of hydrophobic molecules by reducing insolubility and nonuniformity. Ferritin is a multimeric iron storage and detoxification protein and is characterized by its spherical architecture and the internal binding of thousands of

iron atoms.[13-16] Generally, ferritin is characterized by a well-defined hollow cage with inner and outer diameters of 8 and 12 nm, respectively, and is precisely self-assembled from 24 copies of identical or similar subunits that are arranged in an octahedral (432) symmetry to form a spherical protein cage with a large nanocavity (Fig.1B).[17-19] Each ferritin molecule has eight 3-fold channels and six 4-fold channels, through which the inner cavity of ferritin and outside solution is connected.[20] An important, unique characteristic of ferritin, is its reversible assembly, which is reflected by a disassociation of the ferritin cage at pH 2.0/11.0 or addition of denaturants and subsequent reconstitution when pH is adjusted to pH 7.0 or the denaturant is removed.[21,22] During this process, small molecules can be added to a lipid and be captured within the ferritin cage, resulting in the nano-composites.[23,24] An obvious advantage of this method is that the obtained soluble nanocomposites are usually homogeneous in size ~12 nm. However, the encapsulation of water-insoluble small molecules by ferritin is rare reported, possibly because of the different polarities and the incompatibility of the water-insoluble molecules and ferritin cages. Thus, to find the effective method to make them coexist in a same system during the reversible assembly of the ferritin is highly expected.

The aim of this study was to prepare the soluble homogeneous ferritin stabilized rutin nanodispersions (FRNs) by the revisable assembly of the ferritin cage. Characterization of the FRNs included measuring encapsulation efficiency, thermal degradation UV degradation, and release kinetics of rutin during storage. These novel FRNs exhibited significantly improved waster solubility, and showed characteristics which demonstrate that ferritin could be potentially used as a novel vehicle to protect and stabilize water-insoluble molecules.

Material and methods

Isolation and purification of soybean seed ferritin

Dried soybean (Glycine max) seeds were obtained from the local market. Soybean seed ferritin (SSF) was extracted and purified as previously described.[25,26] Apo-soybean seed ferritin (apoSSF) was prepared according to the reported method.[27]

SDS-PAGE was performed to examine the purity of the protein under reducing conditions using 15% gels according to a reported method.[28] The molecular weights of apoSSF were estimated by native PAGE using an 8 % polyacrylamide gradient gel employing Tris-HCl (25 mM, pH 8.3) as running buffer, and the electrophoresis was run at 5 mA for 15 h, at 4 °C. Gels were stained with Coomassie Brilliant Blue R-250. Ferritin concentration was determined according to the Lowry method using bovine serum albumin as standard.[29]

Preparation of FRNs

Rutin (Solarbio Science &Technology Co., Ltd., Beijing, China) (20.0 mg) was dissolved in an ethanol-water solution (80:20, v/v) to make a stock solution with a final concentration of 323.0 μM and stored in the dark in an amber bottle at 4°C. 3.72 mL of rutin stock solution was added to apoSSF solution (2.0 μM, 5.0 mL) with a mole ratio of apoSSF/rutin to be 1:120. The pH value of the resultant solution was adjusted to ~11 with NaOH (1 M) to disassemble ferritin into subunits, and the reaction solution was stirred slowly for 25 min (20 °C). The pH of the resulting mixture was decreased to 7.5 with HCl (1.0 M), followed by incubation at 4°C for 2 h to induce the reassembly of the ferritin cage. The solution was then dialyzed (MW 1000 kDa cutoff) against Tris–HCl buffer (50 mM pH 7.5) six times every 6.0 h intervals to remove free rutin. During dialysis unbound rutin diffuses across the dialysis membrane whilst the encapsulated rutin remains trapped inside of the ferritin cavity due to the narrow ferritin channels (0.3 nm in diameter). Finally, the suspension was further filtered through 0.45-μm hydrophilic cellulose membrane filters to clarify FRNs and then stored at 4°C. The encapsulation efficiency (%) and the loading efficiency (%) are calculated according to Eq. (1) and (2), as follows.

$$\text{Encapsulation efficiency (\%)} = \text{Encapsulated rutin/Total rutin added} \times 100\% \quad (1)$$

$$\text{Loading efficiency (\%)} = \text{Encapsulated rutin/Ferritin} \times 100\% \quad (2)$$

Transmission Electron Microscopy Analyses

Ferritin and FRNs liquid samples were diluted in 50 mM Mops buffer (pH 7.5) prior to placing on carbon-coated copper grids and excess solution removed with filter

paper. Then, Ferritin and FRNs were stained with 2% uranyl acetate for 5 min. and were imaged at 80 kV through a Hitachi H-7650 electron microscope.

UV-Vis spectrum

The UV-Vis spectrums of the rutin and FRNs samples were performed in scanning mode from 210 to 600 nm on an Agilent 8453 spectrophotometer (Agilent, USA). Experiments were carried out in triplicate, and the spectrum data were averaged.

HPLC analysis of rutin

A SSI/LabAlliance HPLC system (Scientific Systems, Inc., PA, USA) consisted of an UV detector (360 nm) and a Waters Xterra RP18 column (4.6×250mm, 5μm) (Waters Corporation, MA, USA). Samples were eluted by the use of a gradient mobile phase consisting of Acetonitrile /water/ methanoic acid (49.6:49.6:0.8, v/v/v) (solvent A) and water/methanoic acid (99.3:0.7, v/v) (solvent B). Gradient conditions were as follows: 0–7 min, 5-30% A; 7–27 min, 30-40% A; 27–30 min, 40-70 % A; 30–33 min, 70-80% A; 33-42 min, 80-100% A; 42–46 min, 100-5% A. The injection volume was 20 μL, and the flow rate of the mobile phase was 0.7 mL/min. To assay the rutin concentration encapsulated in the ferritin cage, samples were adjusted to pH 11.0 by addition of NaOH (1M) to disassemble the spherical structure into subunits, resulting in the release of the rutin. Released rutin was extracted with cyclohexane (2.0 mL) by blending the mixtures up and down in a 5 mL tube for several times, HPLC was applied to determine rutin concentration using rutin as standards (Solarbio Science &Technology Co., Ltd., Beijing, China). This step will be done three times to get the average value of the rutin concentration.

***In vitro* rutin release from FRNs**

Release of the encapsulated rutin was measured using a dialysis based method (MWCO 3500).[30] Specifically, four FRN suspensions (10 mL) with an equivalent rutin concentration of 36.6 μg/mL, were placed in four separate dialysis tubes (MWCO 3500) and dialyzed against 5 L of Tris-HCl buffer (50 mM, pH 7.5) for 15 d at 4°C, 20°C, 37°C, and 50°C in the dark, respectively. Every 24 h, 0.2 mL of the

dialysis buffer was sampled for HPLC to quantify the released rutin. The experiment was performed in triplicate, and the release ratio (%) was calculated according to Eq. (3) as following,

$$\text{Release ratio (\%)} = \text{Released rutin/Encapsulated rutin} \times 100\% \quad (3)$$

Stability of rutin under UV radiation and after thermal processing

To evaluate the stability of rutin encapsulated in ferritin exposed to UV radiation, 10.0 mL of FRN solution (1 μM ferritin, and an equivalent of 30 μM rutin) were placed at a distance of 25 cm under an UV lamp (SW-CJ-1FD Series 20 W UV Lamps, Suzhou, China) with a wavelength of 254 nm for 24 h. Free rutin solution (30 μM) was used as control, 0.4 mL of the solution was sampled once every four hours for HPLC to quantify the remaining rutin.

To assess the thermal stability of rutin in FRNs, 10.0 mL of FRN solution (1 μM ferritin, and an equivalent of 30 μM rutin) were placed in a water bath (Model DK-8D, Tianjin Honour Instrument Co., Tianjin, China) incubated at 37°C or 60°C, respectively, for 24h. The heated samples were assayed every four hours for rutin content by HPLC as described above.

To quantify the kinetics of rutin degradation, data obtained from UV radiation and after thermal processing experiments were fitted to first-order kinetics in Eq. (4) and Eq. (5).

$$C = C_f + (C_0 - C_f)\exp(-kt) \quad (4)$$

$$t_{1/2} = -\ln(0.5)k^{-1} \quad (5)$$

Where C represents the rutin content at different time points; C_f, the rutin content in equilibrium state; C_0, the initial rutin content; k, the degradation rate constant (h^{-1}), and t represents the reaction time (h). The half-life ($t_{1/2}$) was calculated as the time required for rutin decaying to 50% of its initial concentration. Experiments were carried out in triplicate, and the rutin content was averaged for analysis.

DPPH radical-scavenging activity

The antioxidant activity of the samples was determined using the method of DPPH radical-scavenging capacity.[12] One milliliter of free rutin, trolox, and FRNs (an

individual concentrations set as 0.015mg/mL, 0.025mg/mL, and 0.035mg/mL, respectively) were added to 3 mL of DPPH (0.04 mg/ml) dissolved in ethyl alcohol solution. An ethanol/water (80:20) solution was used as control sample for rutin absorption detection; and a Tris-HCl buffer (50 mM, pH7.5) and the apoSSF solution (the relevant concentration refer to rutin) were used as control samples for FRNs absorption detection. Absorbance at 517 nm was determined after 1 h incubation at room temperature in the dark, and antioxidant activity was calculated as followings:

$$\text{DPPH radical-scavenging ratio (\%)} = (1-A_e/A_o) \times 100 \quad (6)$$

Where A_o is the absorbance without sample and A_e is the absorbance with sample.

Statistical Analysis

All analyses were performed in triplicate and all data are presented as mean ± standard deviation (SD). Statistical significance between treatments was determined using SPSS10.0 software. The analysis of variance was calculated at 5% or 1% level of significance.

Results and Discussion

Preparation and characterization of apoSSF

Native PAGE resolved the purified apoSSF as a single complex with an approximate molecular weight estimated to be 560 kDa (Fig. 2A), a typical value for plant ferritin.[31] Subsequently, SDS-PAGE was performed to analyze the subunits of apoSSF which were separated as two peptides with an identical ratio, H-2 (28.0 kDa) *versus* H-1 (26.5 kDa), as displayed in Fig. 2B, and is consistent with our previous observations (supporting information),[22,26] indicating a successful preparation.

The encapsulation of rutin within apoSSF

As mentioned above, ferritin is characterized by a well-defined hollow spherical architecture and is precisely self-assembled from 24 copies of similar subunits that are tightly packed resulting in an internal cavity of approximate diameter of 8 nm.[17,32] The apoferritin shell can kept intact upon heating at 80 ℃ for 10 min, indicative of its relatively high thermal stability.[33] In addition, the reversible assembly characteristic of apoferritin at different pH values provides a subtle route for entrapping food organic

nutritional factors or drug components such as rutin. Rutin with bigger size could not pass through the smaller pore size of ferritin. Fig. 3 illustrates the possible process involved in the encapsulation of rutin into apoferritin during its reassembly. The ferritin nanocage of apoferritin can be dissociated into individual ferritin subunits at pH 11.0, then, the subunits reassemble into a cage-like structure at pH 7.0. During this process, rutin molecules are encapsulated and retained within the ferritin cage, resulting in the FRNs (Fig. 3). The rutin size (12.7 Å in length and 6.0 Å in width, at a minimum energy state calculated by *Chembiodraw Ultra 12.0*) is larger than the pore size of the ferritin protein channels (3–4 Å). Thus, once the rutin is encapsulated, the larger encapsulated rutin will be retained within the apoferritin shell.

Characterization of the FRNs

Firstly, the dissolution state of the FRNs in deionized water (pH 7.0) was observed (Fig. 4A), and both the apoSSF and free rutin dissolved in deionized water (pH 7.0) were used as control samples. Results indicated that, compared to the heterogeneous distribution of the rutin in water (Fig. 4A, iii), the solubility of FRNs was greatly improved (Fig. 4A, ii). A typical yellow color was also observed in the FRNs solution, and the naturally water-insoluble rutin becomes water-soluble while maintaining transparency. This outcome is beneficial for applications involving water soluble rutin in food and pharmaceutical industries.

To further characterize rutin encapsulated within the ferritin cage, transmission electron microscopy (TEM) was performed and the morphology of the FRNs formed by the interaction between rutin and ferritin was investigated, and results shown in Fig. 4B indicate that the FRNs was in a homogeneous state, the same as apoSSF. On the other hand, the control sample, apoSSF, revealed obvious black uranium-containing cores within the ferritin cage as uranium can flow into ferritin cavity via channels after negatively stained with uranyl acetate.[26] By contrast, if the rutin molecules were embedded in the apoSSF cage, one would expect that no uranium-containing cores would form within the cavity, because such encapsulation prevents the entrance of uranyl acetate. The right picture in Fig. 4B just showed no such uranium cores within

the protein cavity, indicating that most of the protein cage molecules are embedded with rutin molecules which might prevent the entry of uranyl acetate into the inner cavity of ferritin.

UV/Vis spectrophotometry was performed to confirm the rutin molecules were successfully embedded in the ferritin cage, as shown in Fig. 4C. Four samples, namely free rutin, FRNs, apoSSF (ferritin[1]), and the sample (ferritin[2]) which was obtained by simply mixing rutin with the apoSSF solution at a molecular ratio of 1:120 (apoSSF to rutin) at pH 7.5 under stirring for 2 h, followed by a 24 h dialysis against Tris–HCl buffer solution at pH 7.5. Results showed that there was no visible absorption in UV/Vis spectrum with the resulting apoferritin solution (ferritin[1]and the ferritin[2]) except for the protein's maximal absorption at 280 nm (Fig. 4C, lines blank and green) indicating that, by such a mixing, the rutin molecules did not interact with the ferritin through exterior binding. As for free rutin, it displayed typical absorption peaks at 260nm and 360 nm (Fig. 4C, blue line). In contrast, the FRNs prepared by the reversible assembly of the apoSSF in Fig. 3 not only showed the protein's maximal absorption but also a new visible maximal absorption at about 350 nm (Fig. 4C, red line) which are characteristics of rutin, demonstrating that rutin molecules were encapsulated within protein shell. Analysis of the maximal absorption of free rutin and the FRNs demonstrated a marked difference. Specifically, the free rutin exhibited a maximal absorption at ~260nm and 360nm, while the FRNs sample showed a maximal absorption at around 350 nm, resulting in a blue shift by 10 nm; FRNs also showed another maximal absorption at ~265nm, a middle value between 280 (protein's maximal absorption) and 260 (rutin's maximal absorption). These results suggested a strong interaction occurs between the trapped rutin molecules and amino acid residues located on the inner surface of apoferritin, which is similar to the report about the interaction between ferritin and anthocyanin.[34] Further reason will be discussed in our further work.

Calculation of rutin encapsulation efficiency

To determine the rutin loading efficiency per ferritin cage, HPLC was performed

using 360 nm as a detection wavelength. Specially, we applied the reversible assembly of the ferritin cage to separate rutin from the internal protein cavity. Firstly, the rutin-ferritin solution was adjusted to pH 11.0 by addition of NaOH (1M) to disassemble the spherical structure into subunits, resulting in the release of the rutin which was extracted with cyclohexane (2.0 mL) and HPLC was then used to determine its concentration. A typical HPLC spectrum for rutin is shown in Fig. 4D, showing a retention time of 33 min. A ratio of concentration (concentration versus peak area) of rutin to that of apoSSF was calculated as 30.1:1 (rutin/apoSSF) under the current conditions. This suggests an average of 30 rutin molecules can be encapsulated in a ferritin cage, and the encapsulation efficiency and loading efficiency were calculated as 25.1% and 3.29%, respectively.

In vitro rutin release from FRNs

The permeability of encapsulated rutin out of the ferritin cage, namely, the leakage kinetics of *in vitro* encapsulated rutin from the ferritin cage were evaluated under simulated conditions (20 mM Tris-HCl, pH 7.4 at 4, 20, 37, and 50°C) for 15 days. It was observed that rutin release ratios of FRNs were all less than 25% after 15 days storage at four temperature conditions (Fig. 5). However, a rapid burst release of greater than 20% was observed within 9 d with subsequent release for a remaining 6 days when FRNs were stored at 50°C. As expected, 12.6 ± 2.1% of the rutin was released at 37°C within 15 days, which was less than that at 50°C but higher than that at 20°C (6.9 ± 1.0%). Thus, the entrapment within the ferritin was efficient in retaining the rutin molecules at lower temperatures and with increased storage temperature, the leakage of the rutin also remarkably increased, suggesting that storage below 20°C would be appropriate for FRNs solution preservation. A higher temperature may result in the degradation of the rutin and the loss of the bioactivity.

Previous reports have showed that about 35 % of rutin is retained when complexed within onion-type multilamellar vesicles (MLVs) for 15 days when MLVs were diluted in water.[12] This strategy applied in this study, by reversible dissociation and reassembly characteristic of soybean see ferritin, demonstrated as much as 75 % of

the rutin is maintained within the protein cage. The mechanism that affects the lower rutin release from the ferritin cage compared to other methods upon storage is possibly due to the unique structure of ferritin. The crystal structure of soybean seed ferritin highlights that one ferritin molecule consists of eight 3-fold and six 4-fold channels with pore sizes between 0.3–0.5 nm, which connect the inner cavity to the external solution.[22,35] Although the diameter of the channel is smaller than the size of rutin, the conformation of rutin during storage may change, resulting in leakage of rutin molecules. In this study the majority of rutin was successfully embedded in the cage, suggesting that the conformational change associated with leakage is limited. However, temperature may be a factor influencing rutin release through altering the ferritin pore structure, and the channels have been shown to be sensitive to the changes in temperature.[36,37]

Stability of rutin in ferritin cage after UV radiation and thermal processing

The effects of UV radiation and thermal processing on rutin stability were investigated to evaluate the protective function of the ferritin cage. Firstly, the UV radiation endurance of rutin was evaluated at a wavelength of 254 nm. Results showed that the control sample of free rutin was degraded rapidly at 254 nm, with 75% degradation after 6 h. In contrast, the degradation of ferritin-encapsulated rutin was significantly reduced as compared with free rutin in the same time range (0-6 h). The data of both ferritin-encapsulated rutin and free rutin are fitted to the first-order reaction model as shown in Eq. (4) to obtain the degradation rate constant (k) and half-time of degradation ($t_{1/2}$) which are listed in Table 1. The regression coefficients (R^2) were obtained as 0.976 and 0.993 for ferritin encapsulated rutin and free rutin, respectively, indicating an excellent correlation between rutin degradation and treatment time. The k and $t_{1/2}$ were 0.25 h^{-1} and 40.11 h for the ferritin encapsulated rutin and were 1.10 h^{-1} and 9.09 h for the free rutin (Table 1), which suggested a greatly improved stability against UV radiation for rutin molecules encapsulated within ferritin nanocages.

Samples were treated at 20 and 37°C to investigate the effect of thermal processing

on rutin degradation. The data for both ferritin-encapsulated and free rutin degradation were fitted to the first-order reaction model in Eq. (4), as shown in Table 1. After incubation at 20 °C for 24 h, rutin degradation in the FRNs was significantly lower than that in free ferritin ($P<0.05$), which is reflected by the lower k value (0.29 h^{-1}) and higher $t_{1/2}$ value (34.48 h). The degradation of rutin at 37°C was markedly increased. The k and $t_{1/2}$ were 0.37 h^{-1} and 27.73 h for the ferritin encapsulated rutin and were 1.07 h^{-1} and 9.35 h for the free rutin (Table 1). These results demonstrated that the ferritin cage can significantly improve the thermal stability of rutin.

The primary reason for the protective effect of ferritin for rutin may lie in the heat resistant properties of the protein cage. It has been reported that the ferritin cage showed no denaturation when heated at 80°C for 10 min.[20,33] Similarly the spherical protein shell may effectively insulate the interior from increased external temperature and possibly absorb UV radiation, thus, stabilizing the encapsulated rutin. Alternatively, ferritin may form molecular complexes with these bioactive compounds through hydrophobic interactions or Vander Waals interactions which may contribute to the resistance from degradation.[38,39] A combination of these novel properties may facilitate the application of ferritin cage technology in the food industry.

Antioxidant property of FRNs

Since the encapsulation of rutin within the apoSSF cage contributed to protection against heating and UV radiation, it is also possible that the antioxidant properties of ferritin embedded rutin may be superior to free rutin molecules. Fig. 6 shows a comparison of the antioxidant activities of free rutin, FRNs, and Trolox as measured by the DPPH scavenging capacity assay. The radical-scavenging abilities of the three samples were dependent on the concentration in a range of 0.015-0.035 mg/mL, which was in agreement with the conclusion obtained by Nguyen et al.[9] Our results indicated that the DPPH scavenging capability of Trolox (85.1%, 0.035 mg/mL) was the highest among the three samples, followed by free rutin (71.2%, 0.035 mg/mL) and FRNs (46.1%, 0.035 mg/mL). Similar results were also obtained when the assay was performed at a lower sample concentration (0.015 and 0.025 mg/mL). Although

the rutin molecules were separated by ferritin shell (~2nm) from the solution, a lower DPPH scavenging capability of FRNs was still presented, indicating that ferritin encapsulation retained part of the antioxidant activity of free rutin.

It has been previously reported that DPPH radical-scavenging ability of an antioxidant is thought to be closely associated with its hydrogen-donating ability.[40,41] As discussed earlier, rutin was encapsulated in the ferritin cage in a ratio of 30:1 (rutin/ferritin), and the rutin molecules are physically separated from the external environment by the protein shell (2 nm in thickness). The maintenance of the DPPH radical-scavenging ability in FRNs, namely, the insignificant differences between DPPH radical-scavenging abilities of free rutin and FRNs, demonstrated a possible change in its hydrogen-donating capacity as a result of the ferritin-rutin complexation. We propose that this change might result from the hydrogen bonds formed between hydrogen atoms in the hydroxyl groups of rutin with the electro-negative atoms of interior surface of ferritin. Subsequently, the forming hydrogen bonds may weaken the covalent bonds between hydrogen and oxygen in the hydroxyl groups, which in turn may facilitate the hydrogen donation by the hydroxyl groups of rutin.[9] Thus, the improved hydrogen donation ability of rutin in FRNs and weaken effect of the ~2 nm thickness of the shell may be in partially equilibrium, resulting in a lower DPPH radical-scavenging ability of FRNs as compared to free rutin.

Conclusion

In this study, the homogeneous ferritin-stabilized rutin nanodispersions were prepared by the reversible dissociation and reassembly of soybean seed ferritin. By applying this interesting strategy, ferritin could be potentially used as a novel vehicle to entrap, solubilize, and stabilize the water insoluble rutin molecules. It is also shown that the rutin encapsulated in ferritin cage shows different release kinetics depending on the operating temperature. Moreover, these ferritin-stabilized rutin nanodispersions provide rutin molecules with improved thermal and UV radiation stability. Additionally, the antioxidant activity of rutin in the ferritin cage was partly retained as

compared to free rutin molecules. These combined findings will advance the application of rutin in the food and pharmaceutical industries.

Acknowledgement

This work was financially supported by the NSFC (No. 31471701), the China-European research collaboration program (SQ2013ZOA100001), and 2015 Tianjin Research Program of Application Foundation and Advanced Technology.

References

1 S. Savic, K. Vojinovic, S. Milenkovic, A. Smelcerovic, M. Lamshoeft and Z. Petronijevic, *Food Chem.,* 2013, **141**, 4194-4199.

2 A. Baldisserotto, S. Vertuani, A. Bino, D. De Lucia, I. Lampronti, R. Milani, R. Gambari and S. Manfredini, *Bioorg. Med. Chem. Lett.,* 2015, **23,** 264-271.

3 T. Koda, Y. Kuroda and H. Imai, *Nutr. Res.,* 2008*,* **28**, 629-634

4 R. M. Gene, C. Cartana, T. Adzet, E. Marin, T. Panella and S. Canigueral, *Planta Med.,* 1996*,* **62**, 232–235.

5 R. Mauludin, R. H. Müller and C. M. Keck, *Eur. J. Pharm. Sci.,* 2009*,* **36**,502-510.

6 T. P. Sari, B. Mann, R. Kumar, R. R. B. Singh, R. Sharma, M. Bhardwaj and S. Athira, *Food Hydrocolloid.,2015,* **43**, 540-546.

7 M. R. Mozafari, K. Khosravi-Darani, G. G. Borazan, J. Cui, A. Pardakhty and S. Yurdugul, *Int. J. Food Prop., 2008,* **11**, 833-844.

8 K. Miyake, H. Arima, F. Hirayama, M. Yamamoto, T. Horikawa, H. Sumiyoshi, S. Noda and K. Uekama, *Pharm. Dev. Technol, 2000,***5**, 399–407.

9 T. A. Nguyen, A. B. Liu, J. Zhao, D. S. Thomas and J. M. Hook, *Food Chem.,* 2013*,* **136**,186-192.

10 P. Jantrawut, A. Assifaoui and O. Chambin, *Carbohyd. Polym.,* 2013*,* **97**, 335–342.

11 R. Kamel and M. Basha, *Bulletin of Faculty of Pharmacy, Cairo University,* 2013*,* **51**, 261-272.

12 A. Kerdudo, A. Dingas, X. Fernandez and C. Faure, *Food Chem.,* 2014*,* **159,** 12–19.

13 J. Lee, S. W. Kim, Y. H. Kim and J. Y. Ahn, *Biochem.Bioph. Res. Co.,* 2002, **298**,

225–229.

14 E. C. Theil, *Annu. Rev. Nutr.,* 2004, **24**, 327–343.

15 P. Arosio and S. Levi, *Free Radical Bio. Med.,* 2002*,* **33***,* 457–463.

16 E. C. Theil, *J. Nutr.,* 2003, **133***,* 1549S–1553S.

17 P. M. Harrison and P. Arosio, *BBA-Gen. Subjects,* 1996, **1275**, 161–203.

18 J. A. Han, Y. J. Kang, C. Shin, J. S. Ra, H. H. Shin, S. Y. Hong, Y. Do and S. Kang, *Nanomedicine,* 2014*,* **10***,* 561–569.

19 J. Deng, X. Liao, H. Yang, X. Zhang, Z. Hua, T. Masuda, F. Goto, T. Yoshihara and G. Zhao, *J. Biol., Chem.*, 2010, **285**, 32075–32086.

20 G. Zhao, *BBA-Gen. Subjects,* 2010*,* **1800**, 815–823.

21 M. Kim, Y. Rho, K. S. Jin, B. Ahn, S. Jung, H. Kim and M. Ree, *Biomacromolecules,* 2011*,* **12***,* 1629–1640.

22 R. Yang, L. Chen, T. Zhang, S. Yang, X. Leng and G. Zhao, *Chem.Commun.,* 2014*,***50***,* 481–483.

23 G. D. Liu, J. Wang, S. A. Lea and Y. H. Lin, *ChemBioChem,*2006*,* **7***,* 1315–1319.

24 B. Bhushan, S. U. Kumar, I. Matai, A. Sachdev, P. Dubey and P. Gopinath, *J. Biomed. Nanotechnol.,* 2014, **10**, 2950-2076.

25 J. Deng, M. Li, T. Zhang, B. Chen, X. Leng and G. Zhao, *Food Res. Int.,* 2011,**44***,* 33-38

26 R. Yang, L. Chen, S. Yang, C. Lv, X. Leng and G. Zhao, *Chem.Commun.,* 2014*,* **50***,* 2879-2882.

27 A. Treffry, J. Hirzmann, S. J. Yewdall and P. M. Harrison, *FEBS Lett.,* 1992, **302**, 108–112.

28 U. K. Laemmli, *Nature,* 1970*,* **227**, 680–685.

29 O. H. Lowry, N. J. Rosebrough, A. L. Farr and R. J. Randal, *J. Biol.Chem.,* 1951, **193**, 265–275.

30 Q. Zeng, H. Wen, Q. Wen, X. Chen, Y. Wang, W. Xuan, J. Liang and S. Wan, *Biomaterials, 2013,* **34**, 4632-4642

31 C. Li, X. Fu, X. Qi, X. Hu, N. D. Chasteen and G. Zhao, *J. Biol.Chem.,*2009*,* **284***,* 16743–16751.

32 N. D. Chasteen and P. M. Harrison, *J. Struct. Biol.,* 1999, **126**, 182–194.

33 S. Stefanini, S. Cavallo, C. Q. Wang, P. Tataseo, P. Vecchini, A. Giartosio and E. Chiancone, *Arch. Biochem. Biophys.,* 1996, **325**, 58–64.

34 T. Zhang, C. Lv, L. Chen, G. Bai, G. Zhao and C. Xu, *Food Res. Int.,* 2014, **62**,183-192.

35 T. Masuda, F. Goto and T. Yoshihara, *J. Biol. Chem.,* 2011, **276**, 19575-19579.

36 E. C. Theil, X. S. Liu and T. Tosha, *Inorg. Chim. Acta,* 2008, **361**, 868–874.

37 X. Liu, W. Jin and E. C. Theil, *P. Natl. Acad. Sci. USA,*2003, **100**, 3653–3658.

38 L. Chen, G. Bai, R. Yang, J. Zang, T. Zhou and G. Zhao, *Food Chem.,*2014, **149**, 307–312.

39 C. Qian, E. A. Decker, H. Xiao and D. J. McClements, *Food Chem.,* 2012, **132**, 1221–1229.

40 J. Yang, J. Guo and J. Yuan, *LWT - Food Sci. Technol.,* 2008, **41**, 1060–1066.

41 O. A. Chat, M. H. Najar, M. A. Mir, G. M. Rather and A. A. Dar, *J. Colloid Interf. Sci.,* 2011, **355**, 140–149.

Figure Captions

Figure 1. (A) Chemical structure of rutin. (B) Graphic representation of the ferritin structure.

Figure 2. (A) Native PAGE and (B) SDS–PAGE analyses of apoSSF. Lane 1 represents apoSSF and the corresponding molecular mass (kDa) is labeled.

Figure 3. Illustration of the process involved in the encapsulation of rutin molecular into apoferritin. In this case, the protein nanocage of apoSSF is disassembled into individual subunits at pH 11.0, and the subunits reassemble into a cage-like structure at pH 7.0. During this process, rutin molecules are encapsulated in the core of the ferritin cage, and can be retained within the cage.

Figure 4. Characterization of the FRNs. (A) Pictures of different samples including apoSSF (i), FRNs (ii), and free rutin simply mixed with deionized water (iii). (B) TEM of apoSSF and FRNs. Samples were stained using 2% uranyl acetate. Bar in TEM is 100 nm. (C) UV–Vis spectra of rutin, FRNs, and ferritin (ferritin^{1} and ferritin^{2}). Ferritin^{1} represents simple apoSSF solution, and ferritin^{2} was obtained by mixing rutin with the apoSSF solution at a molecular ratio of 1:120 (apoSSF to rutin) at pH 7.5 under stirring for 2 h, followed by a 24 h dialysis against Tris–HCl buffer solution at pH 7.5. (D) HPLC chromatogram of rutin extracted from FRNs. Inset: a standard curve of rutin in ethyl alcohol.

Figure 5. Kinetics of rutin release from FRNs at different storage temperatures.

Figure 6. Antioxidant activities of Trolox, rutin, and FRNs by the DPPH radical scavenging method at different concentrations. Each point represents the mean of DPPH radical-scavenging ratio and standard deviation. *P<0.05, **P<0.01.

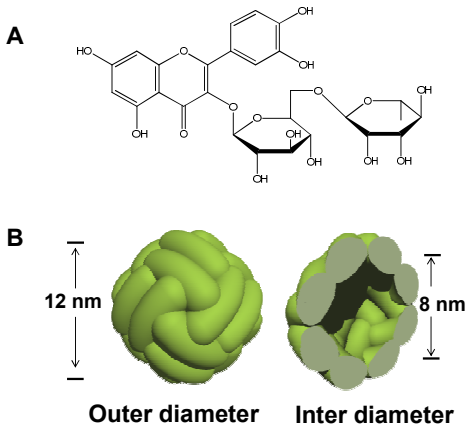

Figure 1

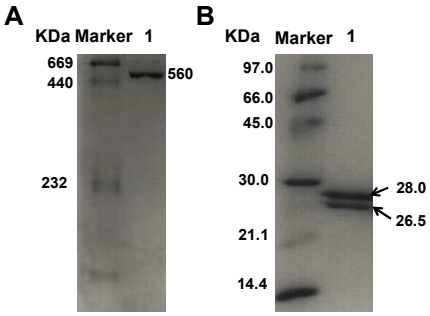

Figure 2

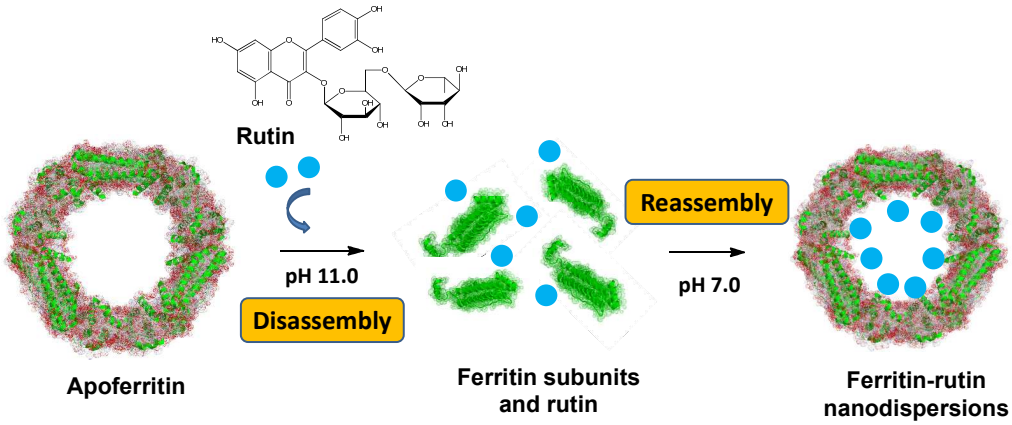

Figure 3

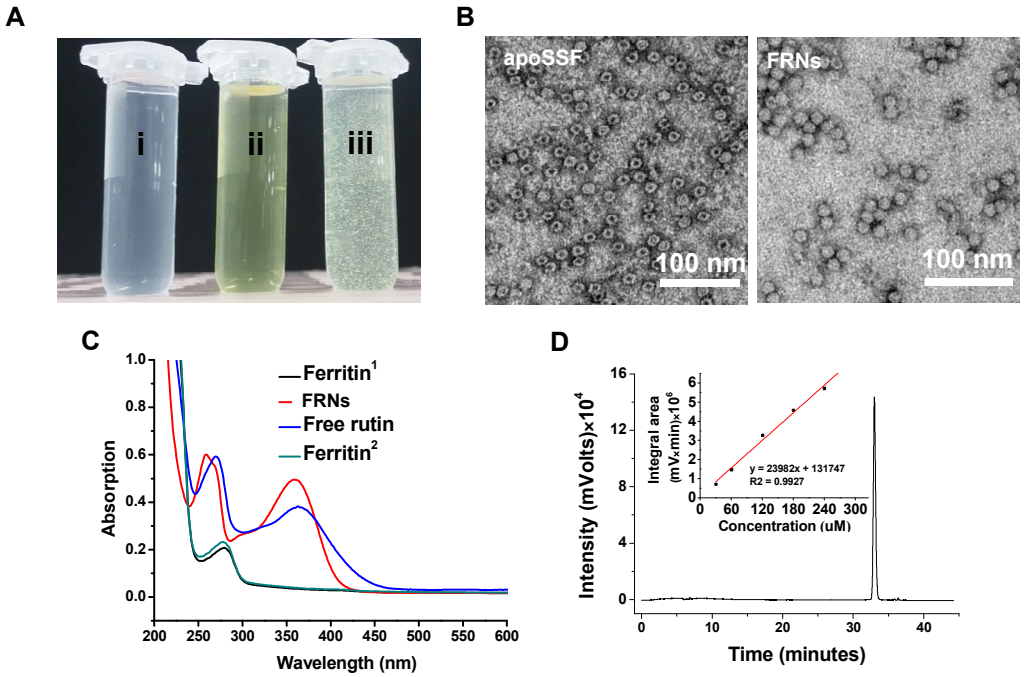

Figure 4

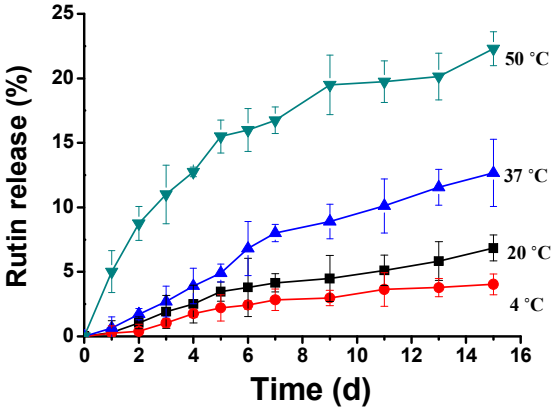

Figure 5

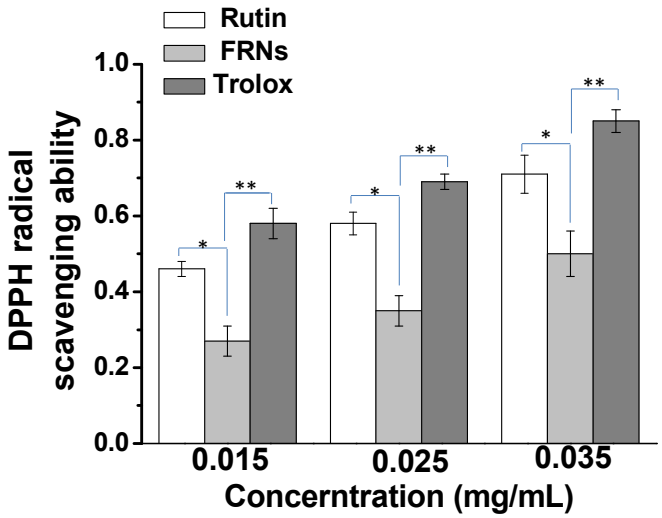

Figure 6

Table 1. Degradation rate constant (k), half-life ($t_{1/2}$), and R^2 when fitting the degradation data of rutin encapsulated in ferritin cage at different conditions.

Treatment	Samples	k(h^{-1})	$t_{1/2}$(h)	R^2
UV radiation (254 nm)	FRNs	0.25 ± 0.03^a	40.11 ± 1.20^a	0.976
	Free rutin	1.10 ± 0.04^b	9.09 ± 0.17^b	0.993
Thermal processing (20 °C)	FRNs	0.29 ± 0.01^a	34.48 ± 1.03^a	0.979
	Free rutin	0.56 ± 0.05^b	17.86 ± 0.99^b	0.983
Thermal processing (37 °C)	FRNs	0.37 ± 0.01^a	27.03 ± 0.90^a	0.966
	Free rutin	1.07 ± 0.03^b	9.35 ± 0.48^b	0.990